POLAR FIELD PUZZLE: SOLUTIONS FROM FLUX-TRANSPORT DYNAMO AND SURFACE TRANSPORT MODELS

MAUSUMI DIKPATI

High Altitude Observatory, National Center for Atmospheric Research [1]; 3080 Center Green, Boulder, Colorado 80301; dikpati@ucar.edu

ABSTRACT

Polar fields in solar cycle 23 were about 50% weaker than those in cycle 22. The only theoretical models which have addressed this puzzle are surface transport models and flux-transport dynamo models. Comparing polar fields obtained from numerical simulations using surface flux transport models and flux-transport dynamo models, we show that both classes of models can explain the polar field features within the scope of the physics included in the respective models. In both models, how polar fields change as a result of changes in meridional circulation depends on the details of meridional circulation profile used. Using physical reasoning and schematics as well as numerical solutions from a flux-transport dynamo model, we demonstrate that polar fields are determined mostly by the strength of surface poloidal source provided by the decay of tilted, bipolar active regions. Profile of meridional flow with latitude and its changes with time have much less effect in flux-transport dynamo models than in surface transport models.

Subject headings: Sun: magnetic field, Sun: activity, Sun: dynamo

1. Introduction

Observations from various instruments indicate that the polar fields in cycle 23 were so weak (see figure 1 of Wang, Robbrecht & Sheeley (2009), see also figure 2 of Arge et al (2002) and figure 2 of Janardhan, Bisoi & Gosain (2010)) that it took a relatively long time to reverse the magnetic polarity of the Sun's North and South poles. Even after the

[1]The National Center for Atmospheric Research is sponsored by the National Science Foundation.

Sun's polarity reversal the build-up of the polar fields was slow (Dikpati et al 2004), resulting in unusually weak polar fields at the end of cycle 23 compared to those in cycles 21 and 22. In order to understand the cause of such a weak polar field at the end of cycle 23 and its consequences for the solar-terrestrial environment, many scientists have extensively employed simulations from flux-transport dynamo models (Dikpati & Charbonneau 1999; Dikpati, de Toma & Gilman 2008; Dikpati et al 2010) and surface transport models (Wang, Lean & Sheeley 2005; Schrijver, De Rosa & Title 2002; Schrijver & Liu 2008).

In both these classes of models the polar fields originate from the decay of tilted, bipolar active regions, namely the so-called Babcock-Leighton mechanism (Babcock 1959; Leighton 1964). The ingredients (advection and diffusion) that directly influence the latitudinal transport of the radial fields in the two classes of models are the same. However, one of the differences in the evolutionary patterns of the polar fields is that, in flux-transport dynamo models, poloidal fields produced at the surface by the Babcock-Leighton effect are axisymmetric (i.e. in the $r-\theta$ plane) and they evolve due to advection and diffusion by the action of both the latitudinal and radial components of the meridional flow as well as by the action of a depth-dependent turbulent diffusivity. By contrast, surface transport models include a more realistic longitude dependence of the Babcock-Leighton effect in the generation of polar fields, and the radial component of the fields generated evolve at the surface by the action of latitudinal component of the meridional flow and a constant surface diffusivity.

The purpose of this paper is to demonstrate that flux-transport dynamo models and surface transport models, despite some differences in the ingredients, produce remarkably similar response in the polar fields' patterns to the changes in the meridional flow-speed when the same latitudinal profile for the poleward surface flow is used. Given that understanding of the polar fields' behaviour is a key to understanding the recycling of magnetic flux for the operation of a dynamo, and hence the properties of future solar cycles, we also examine in this paper whether there are any inconsistencies or contradictions between these two classes of models when applied to the Sun. The polar field puzzle of cycle 23 has become a far more important issue now that the start of cycle 24 has been sluggish.

We illustrate in simple numerical terms just how sensitive the amplitude of the polar field on the Sun and in models is to changes in the strength of the source of its field, namely the emergence and decay of active regions. We know that the amplitude of cycle 23 was 20% weaker than that of cycle 22. If at the end of a given cycle the polar field has one unit, in the next cycle it takes two units of polar fields coming from the surface poloidal source to reverse the remnant polar field and have the new polar fields reach minus one unit. But if the surface poloidal source is 20% smaller in the new cycle than the previous one, as cycle 23 was compared to cycle 22, there are only 1.6 units of new, negative, polar fields

available that can be used to reverse the old, positive, polar field and establish the new, negative, polar field. This means the new, negative, polar field will be only 0.6 units, or 40% smaller in amplitude than that of the previous cycle. The percentage decline in polar field is, therefore, roughly twice the decline in surface source. The observed decline in polar field between cycles 22 and 23 was about 50%. Thus at the outset most of this change can be explained by the change in surface source, whereas other effects are needed to account for the additional drop of 10%.

For both the surface transport and flux-transport dynamo models polar fields are the follower of a cycle by virtue of their origin, namely the decay of tilted, bipolar active regions, hence in a crude analysis as described above, the 40% reduction in polar fields at the end of cycle 23 might be true for all such models. However, a potential weakness of the reasoning just given above is the assumption of a close relation between the strength of a cycle, as measured by the Wolf sunspot number or sunspot area, and the strength of the surface poloidal source arising from the decay of active regions. That is undoubtedly an oversimplification. It is well known that there is a strong correlation between Wolf number and sunspot area; the latter is what has usually been used to drive flux-transport dynamo models and to compare with model output. As seen for example in figure 1 of Dikpati, de Toma & Gilman (2006) there is a good correlation between sunspot area and average surface magnetic flux, provided both data sets are averaged over at least six solar rotations. So presuming a good correlation between Wolf number and the surface source could be plausible, but recent surface transport models (Wang, Robbrecht & Sheeley 2009) do a better job of estimating the surface source from more detailed distributions of active region sources.

2. Role of meridional circulation in polar fields' evolution

The structure and strength of the meridional circulation influence the strength of the Sun's magnetic fields to some extent, but meridional circulation cannot be the most important factor determining the field strength in flux-transport dynamo models. In flux-transport dynamos (and most other dynamos applied to the sun) the spot-producing toroidal fields are generated by the Sun's differential rotation and the poloidal fields are produced by the action of the so-called α-effect. The α-effect is modeled in different dynamo models in different ways. In Babcock-Leighton type flux-transport dynamo models, such an α-effect arises from the decay of tilted, bipolar active regions that emerge to the surface from below. Thus the two sources of magnetic fields, the differential rotation and a combination of α-effects arising from helical turbulence as well as from the decay of active regions, are primarily responsible for determining the amplitudes of toroidal and poloidal fields, and hence the polar fields.

The primary role of meridional circulation in flux-transport dynamo models is the advective transport of magnetic fields, and hence the structure and strength of the flow are crucial in the dynamo models for determining the timings, namely the duration of a cycle, its rise and fall pattern and the timing of the reversals of the Sun's polar fields (Dikpati & Charbonneau 1999; Dikpati 2004; Dikpati et al 2010). A transport process like meridional circulation in a flux-transport dynamo redistributes the dynamo-generated magnetic flux, a relatively minor effect in creating an increase or decrease of magnetic flux. This is illustrated in Table 1 of Dikpati & Charbonneau (1999) in which it is seen that, if the meridional circulation speed is doubled, the peak polar field changes by only 3%, whereas for the same meridional circulation, increasing the surface poloidal source by a factor 2.5 doubles the peak polar field, and decreasing the surface source by 75% decreases the polar field peak by 89%.

The question we address is how flux-transport dynamo models and surface transport models respond to the changes in the surface poleward flow speed. Detailed calculations show that a surface transport model produces a weaker polar field (Wang, Lean & Sheeley 2005; Schrijver & Liu 2008), while a flux transport dynamo gives a stronger polar field when the poleward surface flow-speed is increased (Dikpati & Charbonneau 1999; Dikpati, de Toma & Gilman 2008). Are these opposite results in conflict? We address, first with qualitative reasoning and schematics and then in the next section with numerical solution from a flux-transport dynamo model, whether this is a true conflict, and if so, what is the physical origin of this conflict.

Figure 1 illustrates three scenarios: (a) and (b) for surface flux transport models and (c) for a flux transport dynamo. The primary difference between figures 1(a) and (b) is the latitude where the surface poleward flow is maximum. Figure 1(a) illustrates what happens to surface flux in the declining phase of a cycle when the meridional flow peaks at 6° as in the model by Wang, Lean & Sheeley (2005); Figure 1(b) illustrates what happens for a meridional flow that peaks at 37.5° (Schrijver, De Rosa & Title 2002). Figure 1(c) shows what happens to polar fields when a meridional circulation profile in the pole-to-equator meridional plane peaks at mid-latitudes $\sim 40°$, as has been used in flux-transport dynamo models by Dikpati & Charbonneau (1999) and Dikpati, de Toma & Gilman (2008).

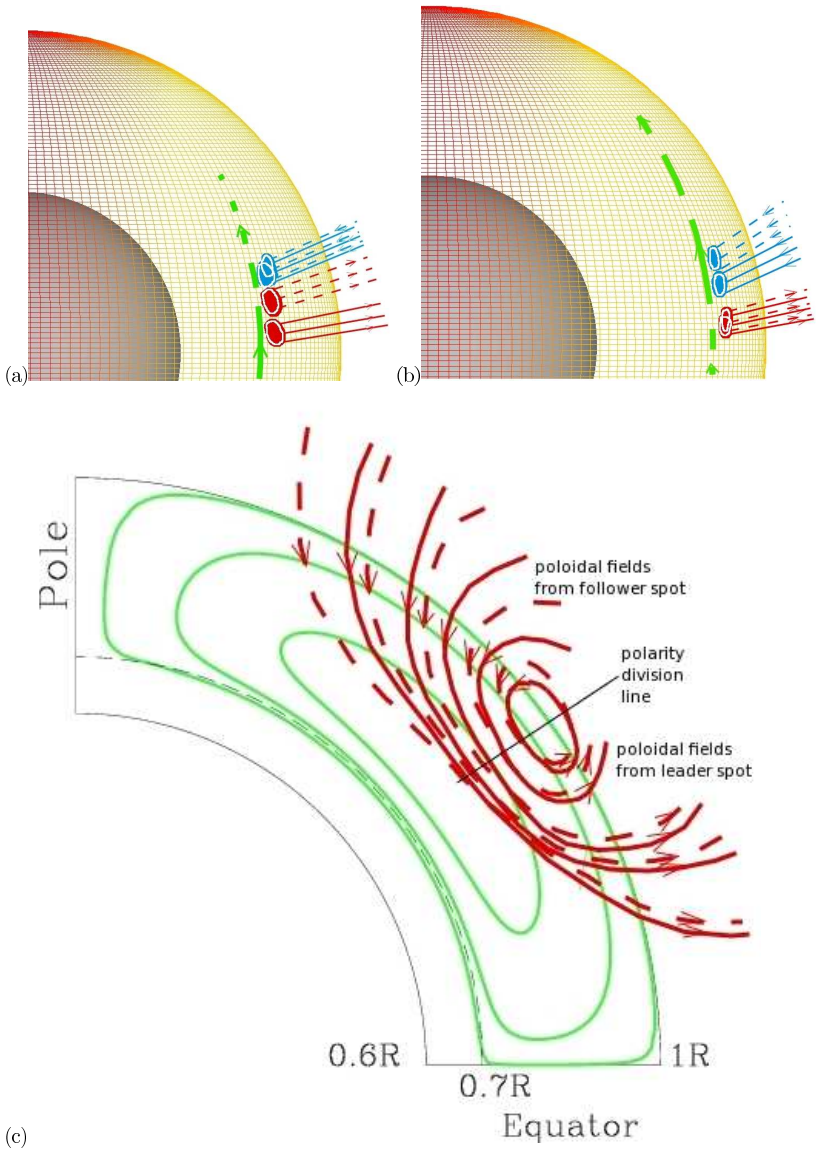

Fig. 1.— Surface radial field transport mechanisms respectively in a surface flux-transport model with a poleward flow peaking at 6° (frame a) as in the model of Wang et al. (2005), the surface transport model with a poleward flow peaking at 37.5° (frame b) as in the model of Schrijver et al. (2002), and in a flux-transport dynamo model with a flow peaking at mid-latitudes (frame c) as in the model of Dikpati et al. (2008). In frames (a) and (b), red and blue patches on the surface represent bipolar active regions. Red and blue continuous lines represent radial fields from a bipole, and dashed lines represent the new locations of radial fields after the meridional flow is increased. For example, by doubling flow speed, a larger increase in transport-rate is obtained respectively on equatorward and poleward side of the bipoles in frames (a) and (b); thus fields from leader polarity drift closer to fields from follower polarity in frame (a) and further apart in frame (b). Frame (c) describes a very similar situation as in frame (b), but in terms of poloidal fields in $r - \theta$ plane. Solid contours represent poloidal fields produced from bipolar active regions and dashed contours represent that for an increased flow. Polarity division line of large-scale poloidal fields from a flux-transport dynamo model is shown by a dark line.

We can understand from Figure 1(a) that, when the flow is maximum at low (6°) latitudes, an increase in poleward flow speed leads to a larger rate of transport on the equatorward side of the leader polarity, and hence a faster poleward transport of the leader polarity compared to the follower polarity. Thus the leader polarity gets closer to the follower polarity to create enhanced annihilation between them. This reduces the fields coming from the follower polarity that reach the pole and thus produce weaker polar fields. This is what has been obtained by Wang, Lean & Sheeley (2005) and Schrijver & Liu (2008) in simulations using surface transport models. On the other hand, when the flow speed is maximum at mid-latitudes (Figure 1(b)), an increase in flow speed leads to a larger rate of transport on the poleward side, causing the follower and the leader polarities to separate more from each other. Thus there is less annihilation between them. Consequently the polar field should increase. Schrijver, De Rosa & Title (2002) explained, using a flow peaking at 37.5°, that the poleward meridional flow is so effective in maintaining the high latitude field that this flow would have to practically disappear to get a significant decay of the polar flux. We can thus infer that, quite consistently a decrease in flow leads to a decrease in polar flux, and increase in flow to an increase in polar flux when the flow peaks at 37.5° latitude.

It follows from the reasoning above that the increase in polar field amplitude with the increase of meridional flow speed in flux-transport dynamo models Dikpati & Charbonneau (1999) and Dikpati, de Toma & Gilman (2008) and surface transport model of Schrijver, De Rosa & Title (2002), and the decrease in polar field with the increase in meridional flow-speed in the surface transport models of Wang, Lean & Sheeley (2005) and Schrijver & Liu (2008), are not in conflict. Rather, it is the choice of meridional flow profile – peaking at low latitudes or at mid-to-high latitudes – that leads to the opposite results which are physically consistent. We recognize that cross-equatorial flux cancellation may also play a role in producing the results of Schrijver & Liu (2008).

There now exist detailed measurements of meridional flow speed by several methods for all of cycle 23, (Ulrich 2010; Basu & Antia 2010; Hathaway & Rightmire 2010) so detailed comparisons can be made. This has been done most extensively in Ulrich (2010). All measurements show significant variations from year to year within cycle 23, some of which appear to correlate with variations in rotation, in particular the torsional oscillations, as seen in the helioseismic results of Basu & Antia (2010). In terms of meridional flow averaged over cycle 23 (see figure 1 of Dikpati, Gilman & Ulrich (2010) and figure 10 of Ulrich (2010)) it is clear that surface Doppler (Ulrich 2010) and helioseismic (Basu & Antia 2010) results agree closely with each other, while the magnetic feature tracking results (Hathaway & Rightmire 2010) are distinctly different. In particular, surface Doppler and helioseismic measures have an average peak at 25° and the peak shifting with time between 15 and 40 degrees, while magnetic feature tracking flow speed peaks closer to 50 degrees and has a distinctly lower

peak value.

Early surface transport models (Devore, Boris & Sheeley 1984; Wang, Nash & Sheeley 1989) were the first to use a latitudinal meridional flow profile peaking at low latitudes, in particular, 6 degrees, even before observations could tell us where the flow peaks. Such a low-latitude peak gave the best fit of model-derived surface features with observations of surface magnetic fields. In future the much more extensive Doppler based observations of meridional flow can be used as input to both surface transport models and flux-transport dynamo models, capturing the low latitude peak now observed. By contrast, the magnetic feature-tracking speed should be compared with the output of such models in order to estimate the surface magnetic diffusivity.

There is a tracking speed that might also be useful as input to dynamo and surface transport models. That is the tracking speed that comes from the Doppler signal of supergranules (Švanda et al 2008). It has been used to measure differential rotation and meridional circulation for solar cycle 23. It will be useful to compare the details of flow profiles obtained by this method with those obtained by more global surface Doppler as well as helioseismic measures.

3. Model calculations

3.1. Polar field simulations from a self-saturated flux-transport dynamo driven by Babcock-Leighton α-effect only

In most flux-transport dynamo models, starting from Dikpati & Charbonneau (1999), the poleward surface flow has generally been taken to be a maximum in midlatitude. So according to the qualitative reasoning given in Figure 1, the fields from the follower polarity separate out from the leader polarity at a faster rate (see Figure 1(c)) when the flow speed is increased. Thus there is less annihilation among them; consequently the polar field increases. To test this with flux-transport dynamo simulations, we must take account of the fact that there are additional physical processes at work in the model that will change the poloidal and toroidal fields in other parts of the dynamo domain in response to a change in meridional flow. For example, if the flow toward the poles at the top speeds up, the return flow near the bottom will also speed up. This bottom flow then moves the poloidal field there faster toward the equator, leaving less time to induce toroidal field at a particular latitude. This reduction in bottom toroidal field in turn leads to a reduced surface poloidal source. Which wins in determining whether the polar fields increase or decrease? In Figure 2a we show results from new simulations with our flux-transport dynamo model using ingredients very similar

to those used in Dikpati & Charbonneau (1999) for a pure Babcock-Leighton dynamo (no bottom α-effect) that answers this question. Figure 2a displays measures of the surface polar field (blue diamonds) and the tachocline toroidal field (black triangles) for a sequence of independent simulations of the self-excited dynamo for different peak meridional flow speeds (all peaking at the same midlatitude). Each simulation is run for about 5 cycles to reach a nonlinear equilibrium in which each successive cycle has the same period and amplitude.

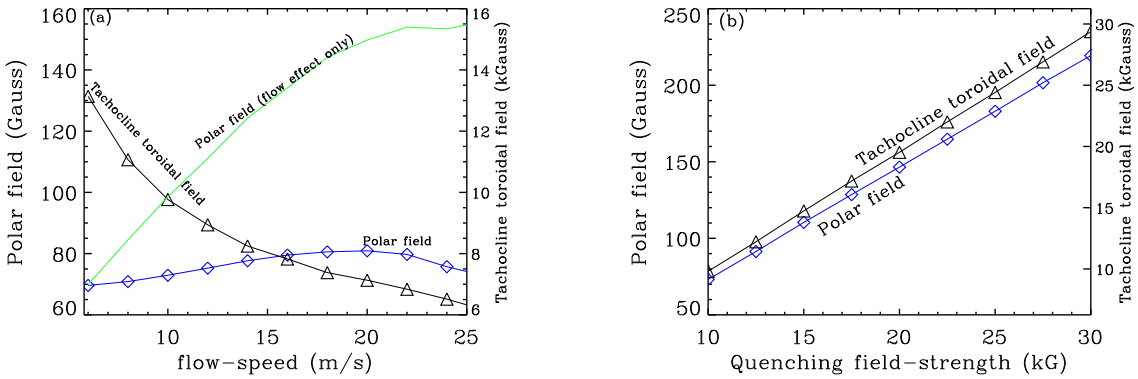

Fig. 2.— (a) Polar fields at $\sim 75°$ (left hand scale, blue diamonds and curve) and tachocline toroidal fields (right hand scale, black triangles and curve) for self-excited Babcock-Leighton flux transport dynamo solutions with different peak flow speeds (horizontal scale). Flow profile used is very similar to that taken in Dikpati & Charbonneau (1999), which peaks at mid-latitudes. Green curve is polar fields normalized to the same tachocline toroidal field for all cases, illustrating polar fields obtained for the same tachocline toroidal fields. (b) Polar fields at $\sim 75°$ and sub-surface tachocline toroidal fields as a function of quenching field strength.

Since the dynamo-generated field strengths depend on the choice of quenching field strength also, we plot in Figure 2b the polar and subsurface toroidal field amplitudes as function of the quenching field strength in the α-effect. We find a nearly linear relationship between the simulated magnetic field amplitudes and quenching parameter. It is not yet possible to know from observations what should be the actual quenching field strength, but to obtain an optimum results of polar as well as subsurface toroidal field values from a Babcock-Leighton flux-transport dynamo, it is conceivable that the quenching field strengths range within 10-30 kGauss. Thus Figure 2(b) implies that the polar and subsurface toroidal fields also be scaled accordingly when a different quenching field strength is used.

We see from Figure 2a that for the example we have chosen, whether the polar field is larger or smaller (blue diamonds and curve) for a larger meridional flow depends on the amplitude of the flow. This effect was also seen in Baumann et al (2004) who, using a

surface transport model, reported non-monotonic behavior of the polar fields as a function of flow-speed. This confirms that surface transport models and flux-transport dynamo models, despite operating with slightly different ingredients, produce similar basic surface radial field features. For flux-transport dynamos, the amplitude of polar fields is affected greatly by the decrease in induced toroidal field at the bottom (black triangles and curve), because this reduces the surface poloidal source from which the polar fields are produced. If we normalize out this effect by adjusting the bottom toroidal fields to the same value for all meridional flow speeds, so the surface poloidal source is independent of meridional flow speed, then the polar field would be given by the green curve. Thus for the same surface source, the polar field does increase markedly with an increase in meridional flow speed for the choice of flow profile that peaks at mid-latitudes, consistent with the schematic description provided in Figure 1.

One important issue about a flux-transport dynamo driven by a Babcock-Leighton α-effect is that it cannot really reproduce a best match of polar field amplitudes with observations. This fact has been noted by many Babcock-Leighton dynamo modelers since early 1990's (Durney 1995, 1996, 1997; Dikpati & Charbonneau 1999). In some attempts for reproducing a correct polar field value using such models, the dynamo has actually died after a few cycles, because a recycled polar flux of only ten Gauss is not enough to maintain the dynamo, for example see the discussion of Table IV of Dikpati et al (2002). That consideration led to the development of a calibrated flux-transport dynamo driven by a small amount of the tachocline α-effect in addition to a Babcock-Leighton α-effect, results from which we discuss next.

3.2. Simulations from a calibrated flux-transport dynamo with sudden change in meridional flow-speed

We carry out further numerical simulations making a sudden change in meridional flow in the model and finding the change in the polar field in the first one or two cycles that follow. This is done for the case of a self-excited flux-transport dynamo that achieves saturation only by 'alpha-quenching-like' amplitude-limiting nonlinearity, run with a steady meridional flow and with the fixed dynamo source terms. In this case, for a given set of input parameters, the model produces all cycles of the same amplitude.

Starting from such a saturated dynamo solution, we do numerical experiments for peak meridional circulation amplitudes ranging from $6 - 32\,\mathrm{ms}^{-1}$ for two distinct circulation profiles, one peaking at 25° as used in Dikpati et al (2010a), and the other peaking at 50°. Following expression (1) of Dikpati et al. (2010a), we prescribe a meridional flow profile as:

$$\psi r \sin\theta = \psi_0(\theta - \theta_0) \sin\left[\frac{\pi(r - R_b)}{(R - R_b)}\right] \left(1 - e^{-\beta_1 r \theta^\epsilon}\right) \left(1 - e^{\beta_2 r(\theta - \pi/2)}\right) e^{-((r-r_0)/\Gamma)^2}, \qquad (1)$$

in which, $R_b = 0.69R$, ${\beta_1}^2 = 0.1/(1.09 \times 10^{10})\,\mathrm{cm}^{-1}$, $\beta_2 = 0.3/(1.09 \times 10^{10})\,\mathrm{cm}^{-1}$, $\epsilon = 2.00000001$, $r_0 = (R - R_b)/5$, $\Gamma = 3 \times 1.09 \times 10^{10}\,\mathrm{cm}$ and $\theta_0 = 0$. This choice of the set of parameter values produce a flow pattern that peaks at 24° as shown in the blue curve in Figure 3(a). The dimensionless length in our calculation is $1.09 \times 10^{10}\,\mathrm{cm}$ and the dimensionless time is $1.1 \times 10^8\,\mathrm{s}$, which respectively come from taking the dynamo wavenumber, $k = 9.2 \times 10^{-11}\,\mathrm{cm}^{-1}$, as one dimensionless length, and the dynamo frequency, $\nu = 9.1 \times 10^{-9}\,\mathrm{s}^{-1}$, as one dimensionless time. In other words, the dynamo wavelength ($2\pi \times 1.09 \times 10^{10}\,\mathrm{cm}$) is 2π and the mean dynamo cycle period (22 years) is 2π in our dimensionless units. Thus, in nondimensional units, the above parameters are: $R_b = 4.41$, $\beta_1 = 0.1$, $\beta_2 = 0.3$, $\epsilon = 2.00000001$, $r_0 = (R - R_b)/5$, $\Gamma = 3$ and $\theta_0 = 0$. Thus in nondimensional units, by changing β_1 from 0.1 to 0.8 and β_2 from 0.3 to 0.1, a flow pattern peaking at 50° can be obtained. This means the dimensional values for β_1 and β_2 will be $\beta_1 = 0.8/(1.09 \times 10^{10})\,\mathrm{cm}^{-1}$ and $\beta_2 = 0.1/(1.09 \times 10^{10})\,\mathrm{cm}^{-1}$ in order to create a poleward surface flow peaking at 50°, as shown in the red curve in Figure 3(a).

Here $\rho(r) = \rho_b[(R/r) - 0.97]^m$, with $m = 1.5$ and ρ_b taken as 1 gm/cc for practical purposes. Then using the constraint of mass-conservation, the velocity components can be obtained as, $v_r = \frac{1}{\rho r^2 \sin\theta} \frac{\partial}{\partial\theta}(\psi r \sin\theta)$ and $v_\theta = -\frac{1}{\rho r \sin\theta} \frac{\partial}{\partial r}(\psi r \sin\theta)$.

All other ingredients (α-effects, differential rotation, and quenching) remain the same as in Dikpati et al (2010). In both cases the peak velocity before the abrupt change is 18 m/s, which is set by adjusting the values of ψ_0. In both cases, $\theta_0 = 0$ ensures that there is a single meridional flow cell that extends all the way to the poles from the equator. In all cases, the change in meridional flow is timed to occur at the epoch of polar reversal. We get similar results if the change in flow speed occurs at other phases of a cycle.

The polar field amplitude produced by the model for all these cases is plotted in Figure 3(b). This amplitude is the maximum, area weighted average of the radial field from 55° latitude to the pole for the first polar field peak to occur after the change in meridional flow speed (the same average as used in Dikpati et al (2010)). We see in Figure 3(b) that the amplitude of the change in polar fields with a sudden change in meridional flow is rather

[2]The parameter values for β_1, β_2 and Γ were given in dimensionless units in the GRL paper by Dikpati et al. (2010a), whereas other parameters were given in dimensional units; we thank Dr. Luis Eduardo Antunes Vieira for helping us catching that.

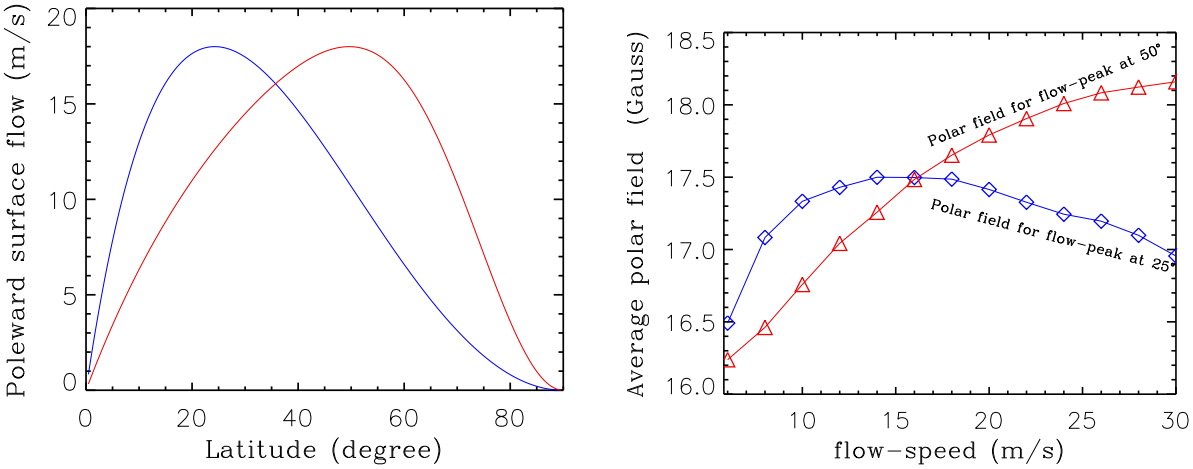

Fig. 3.— (a) Typical profiles of poleward surface flow in meridional circulation used in set of self-excited flux transport dynamo simulations; blue curve from Dikpati et al (2010a) with peak near 25°; red curve a profile with peak near 50°. (b) Polar field amplitudes in the polar cap (latitudes 55° to 90°) from model simulations, for cycle immediately following sudden change in meridional flow speed from 18 m/s to value shown on horizontal axis. Nine Gauss has been added to the red curve so it can be compared to the blue curve on the same scale. The much lower actual polar fields in the red curve are probably caused by the longer transport time from the source in active latitudes to the poles, since the meridional flow peaks at a much higher latitude in this case.

small – no more than 10% for the full range of circulation amplitude change for either profile, perhaps within the measurement error for average polar fields. Thus the sudden change in meridional flow has little effect on the polar field peak in the cycle immediately following the change. Thus in a flux-transport dynamo model, a change in peak polar fields of as much as several tens of percent between one cycle and the next can not come from a change in meridional flow speed. It must come from a significant change in the amplitude of the source of polar fields, namely the eruption and decay of active region magnetic flux.

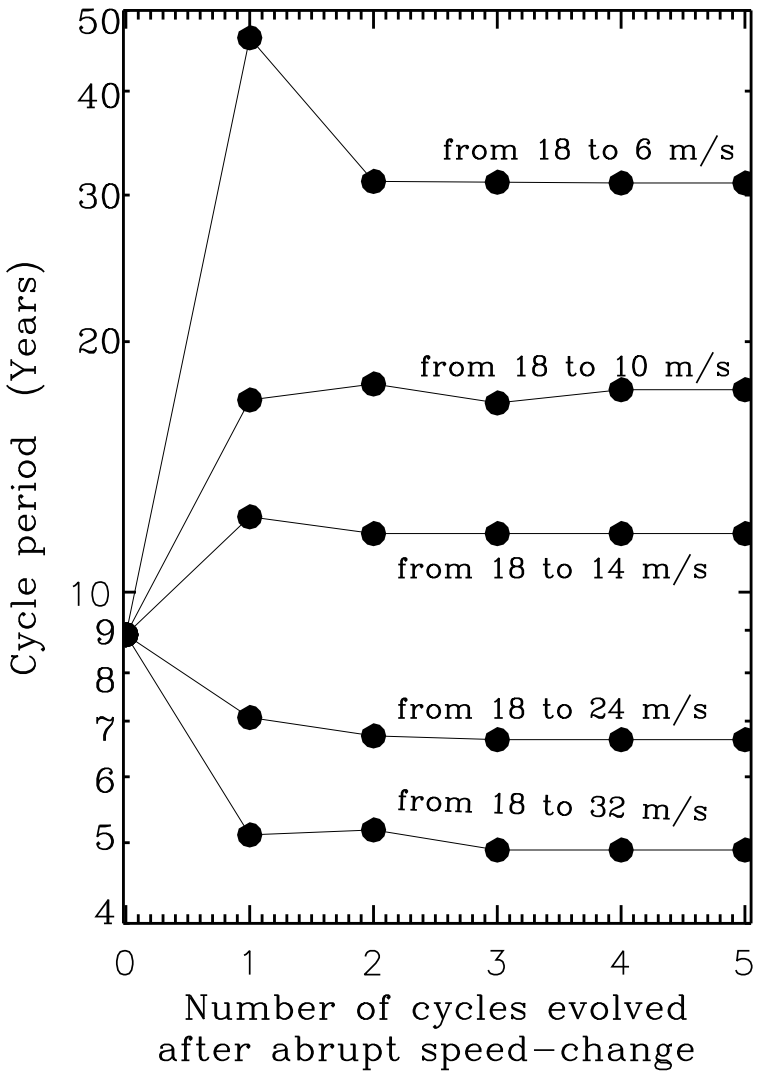

Fig. 4.— Periods of first five cycles following a sudden change in meridional flow speed in a flux-transport dynamo model. The period sequence from each simulation is marked with the amount of the change. All simulations start from a previous simulation with peak meridional flow speed of $18\,\mathrm{ms}^{-1}$, which gives a period of about 9 years, shown on the left hand scale for cycle number zero.

How the polar field maximum of the next cycle changes with the change in meridional flow is quite different for the two profiles. For the low latitude peak in flow, both faster and slower meridional flow leads to a decrease in polar field strength, while for the high latitude flow peak, the faster(slower) the new flow, the larger (smaller) subsequent polar field peak. The changes in polar field that occur for an increase in meridional flow speed for the two meridional flow profiles are completely consistent with the qualitative arguments made using Figure 1 of §2. So is the decline in polar field when the meridional circulation with high latitude peak is reduced. Only the decline in polar fields when the flow pattern peaking at low latitudes is reduced requires a different explanation – perhaps the dynamo cycle-period gets so long that there is more time for the surface flux moving to the poles to be diffused down and not reach the pole.

These simulations of changes in polar fields due to drastic changes in meridional circulation raise lead to an additional question – how quickly does the dynamo period adjust to the changed meridional flow. Figure 4 plots the period of the first five cycles computed following the abrupt change in meridional flow speed without altering the form of the streamlines. Not surprisingly, the new periods are about what we would expect for an advection-dominated flux-transport dynamo in which the dynamo cycle-period is inversely proportional to the meridional flow-speed. What is perhaps surprising about the results seen in Figure 4 is how quickly the model adjusts to the new period established by the changed meridional flow. Except for the extreme case when the flow peak is reduced from $18\,\mathrm{ms}^{-1}$ to $6\,\mathrm{ms}^{-1}$, we see that the adjustment occurs almost entirely within the first cycle. A forthcoming paper on sequential data assimilation for solar dynamo models is addressing this issue in more detail; preliminary results indicate that the 'response time' of a flux-transport dynamo to a change in meridional flow is as short as about 8 months.

The Figure 4 shows the settlement of the dynamo cycle-period for a calibrated dynamo as discussed in§3.2. For a pure Babcock-Leighton flux-transport dynamo as in Dikpati & Charbonneau (1999), without any tachocline α-effect, the cycle-period changes in a similar way. However, for the same meridional flow-speed the cycles are little faster in that case.

In diffusion-dominated dynamos the cycles are faster than that in advection-dominated dynamos, due to enhanced diffusive transport added to the advective transport of magnetic flux. An extensive analysis by Hotta & Yokoyama (2010) shows how the dynamo cycle-period would change when the magnetic diffusivity in the bulk of the convection zone is increased. From the above study we anticipate that diffusion-dominated dynamos would respond to a sudden change in meridional flow-speed in an analogous way to that seen in Figure 3(b). However, it would be worthwhile in the future to do an investigation of the response of advection-dominated dynamos of Muñoz-Jaramillo et al (2010) that used a more

sophisticated buoyancy mechanism than was used by Dikpati & Charbonneau (1999).

4. Discussion

While both surface flux-transport models and flux-transport dynamo models include the advective-diffusive transport of magnetic flux, and both can consistently explain polar field patterns, there are inherent differences – surface transport models simulate the evolution of radial fields on the photospheric latitude-longitude surface, whereas flux transport dynamo models solve the axisymmetric dynamo equations for the toroidal field, B_T, and the vector potential, A ($\nabla \times A$ represents poloidal fields) in the meridian plane in the convection zone. There are additional physical effects operating in the evolution of magnetic fields in a flux-transport dynamo model, due to the presence of the radial flow in the circulation pattern, radial diffusion, and depth-dependent diffusivity. Similarly additional physical effects are captured in surface transport models, namely their more realistic treatment of longitude dependence and hence estimation of the Babcock-Leighton surface source term for poloidal and therefore polar fields.

When poleward surface flow is increased in a flux-transport dynamo, if there is no change in the profile of meridional flow, the upward flow near the equator and the downward flow near the high-latitudes will also increase, causing the poloidal fields produced from the leader polarity to move up to a slightly higher diffusivity region compared to where they would have been if the flow would not have increased. The poloidal fields from the follower spots, on the other hand, do the opposite — they sink down towards the lower diffusivity region (see Figure 1c). As a consequence, the equatorward side of the polarity division line of those poloidal fields undergoes faster diffusive decay, while the poleward side undergoes less decay and therefore remains more frozen. Since the dynamo equations solve for the vector potential, A, the changes in A described above get reflected in the radial component of the poloidal field, given by $\frac{1}{r^2 \sin\theta}\frac{\partial}{\partial\theta}(A\, r\, \sin\theta)$. Thus the presence of depth-dependence in the diffusivity profile and the radial component in the meridional flow profile both contribute to the increase in the poloidal fields on the poleward side of the bipoles. This effect is not present in surface transport models.

Nevertheless, we have shown through physical description and numerical calculations that the surface flux-transport models and flux-transport dynamo models, despite some differences in their physics, produce similar results when run with a very similar latitudinal profile of surface poleward meridional flow, although surface-transport models can better reproduce polar field patterns in latitude and time compared to any dynamo model.

As a consequence of the absence of depth-dependent diffusivity, the radial component of the meridional flow and the latitudinal component of the poloidal fields, surface-transport models produce a more visible difference in the polar field amplitudes than the polar fields obtained from a flux-transport dynamo model when a high-latitude reverse flow-cell is present. Jiang et al (2009) have shown that the surface radial fields get significantly reduced at the pole if the poleward surface flow reverses beyond 70°. However, flux-transport dynamo models change the latitude location of the maximum surface radial fields from pole to the boundary of the two cells when such models are run with two flow cells (Bonanno et al 2005; Jouve & Brun 2007; Dikpati et al 2010). The observed polar fields from Wilcox Solar Observatory are instrumentally averaged over the latitude range from 55° to the pole. Thus the model-derived radial fields integrated over the latitudes from 55° up to the pole and weighted by the surface area, (i.e. $< B_r >= \frac{\int_0^{2\pi}\int_0^{2\pi/5.143} B_r R^2 \sin\theta d\theta d\phi}{\int_0^{2\pi}\int_0^{2\pi/5.143} R^2 \sin\theta d\theta d\phi}$) are not actually much different in the two cases whether a high-latitude reverse-cell is present or absent (see the discussion in (Dikpati et al 2010)).

In this analysis, we confined ourselves to consideration of advection-dominated flux-transport dynamos and surface transport models. How polar fields respond to changes in meridional flow in the cases of diffusion-dominated dynamos (Yeates, Nandy & Mackay 2008) and flux-transport dynamos with more complexities included, such as turbulent pumping (Guerrero & de Gouveia Dal Pino 2008), diffusivity quenching (Guerrero, Dikpati & de Gouveia Dal P 2009) and buoyancy-induced delay in surface poloidal field generation (Jouve, Proctor & Lesur 2010), have not yet been explored.

An alternative explanation for the weak polar fields and long minimum of cycle 23 has been given by Nandy, Muñoz-Jaramillo & Martens (2011). Using an advection-dominated flux-transport dynamo (Muñoz-Jaramillo, Nandy & Martens 2009) that operates with a two-step diffusivity profile, Nandy, Muñoz-Jaramillo & Martens (2011) do a large number of simulations in which the meridional flow amplitude is changed randomly, once per cycle, at cycle maximum. The peak amplitude falls in the range of $15 - 30\,\mathrm{ms}^{-1}$. They find that cycles in which the meridional flow speed is larger in the ascending phase than in the declining phase tend to be followed by longer, deeper minima, and the polar field strength of such cycles tend to be weaker. Both these correlations are modest, with correlation coefficient $r \sim 0.5$, which corresponds to a variance of one-quarter only. This means that the other 75% of the variance in polar fields' weakening must be due to other effects. In addition, no observational evidence was given in Nandy, Muñoz-Jaramillo & Martens (2011) that the meridional circulation in cycle 23 actually was higher in the ascending phase than in the descending phase, and, indeed, the best measures of surface plasma flow for cycle 23 that exists, namely that of Ulrich (2010) and Basu & Antia (2010), does not support the as-

sumption of speed-up in meridional flow-speed in the ascending phase of cycle 23 (see figure 6 of Ulrich (2010) and figure 3 of Basu & Antia (2010)). Thus it follows that, at least for cycle 23, it is not possible to explain the polar field drop or the long minimum using the correlation found by Nandy, Muñoz-Jaramillo & Martens (2011).

Currently all benchmarked flux-transport dynamos operate in the 2D axisymmetric regime (see Jouve et al (2008)). It is also necessary to investigate the role of longitude-dependence from the tilted, bipolar active regions in the generation of evolution of the Sun's polar fields using a 3D version of flux-transport dynamos.

5. Acknowledgements:

We thank Peter Gilman for reviewing the manuscript. We extend our thanks to an anonymous referee for helpful comments which helped improve the manuscript. This work is partially supported by NASA's Living With a Star program through the grant NNX08AQ34G. The National Center for Atmospheric Research is sponsored by the National Science Foundation.

REFERENCES

Arge, C. N., Hildner, E., Pizzo, V. J. & Harvey, J. W., 2002, Journal Geophys. Res., 107(A10), 1319.

Babcock, H. D. 1959, ApJ, 130, 364.

Basu, S. & Antia, H. M. 2010, ApJ, 717, 488.

Baumann, I., Schmitt, D., Schüssler, M. & Solanki, S. K., 2004, A&A, 426, 1075.

Bonanno, A., Elstner, D., Belvedere, G. & Rüdiger, G. 2005, AN, 326, 170

Charbonneau, P. 2007, Adv. in Space Res., 39, 1661.

Devore, C. R., Boris, J. P. & Sheeley, N.R., Jr. 1984, SolP, 92, 1.

Dikpati, M. & Charbonneau, P., 1999, ApJ, 518, 508.

Dikpati, M., Corbard, T., Thompson, M. J. & Gilman, P. A., 2002, ApJ, 575, L41.

Dikpati, M., 2004, ESA-SP, 559, 233

Dikpati, M., de Toma, G., Gilman, P. A., Arge, C. N. & White, O. R., 2004, ApJ, 601, 1136.

Dikpati, M., de Toma, G. & Gilman, P. A., 2006, Geophys. Res. Lett., 33, L05102.

Dikpati, M., de Toma, G. & Gilman, P. A., 2008, ApJ, 625, 920.

Dikpati, M., Gilman, P. A., de Toma, G. & Ulrich, R. K., 2010, Geophys. Res. Lett., 37, L14107.

Dikpati, M., Gilman, P. A. & Ulrich, R. K., 2010, ApJ, 722, 744.

Durney, B. R., 1995, SolP, 160, 213

Durney, B. R., 1996, SolP, 166, 231

Durney, B. R., 1997, ApJ, 486, 1065

Guerrero, G. M. & de Gouveia Dal Pino, E. M. 2008, A&A, 485, 267

Guerrero, G. M., Dikpati, M. & de Gouveia Dal Pino, E. M. 2009, ApJ, 701, 725

Hathaway, D. H. & Rightmire, L. 2010, Science, 327, 1350

Hotta, H. & Yokoyama, T. 2010, ApJ, 714, 308

Janardhan, P., Bisoi, S. & Gosain, S., 2010, SolP, 267, 267.

Jiang, J., Cameron, R., Schmitt, D. & Schüssler, M., 2009, ApJ, 693, L96

Jouve, L. & Brun, A. S. 2007, A&A, 474, 239

Jouve, L., Brun, A. S., Arlt, R., Brandenburg, A., Dikpati, M., Bonanno, A., Käpylä, P. J., Moss, D., Rempel, M., Gilman, P., Korpi, M. J. & Kosovichev, A. G. 2008, A&A, 483, 949

Jouve, L., Proctor, M. R. E. & Lesur, G. 2010, A&A, 519, 68

Leighton, R. B. 1964, ApJ, 140, 1547

Muñoz-Jaramillo, A., Nandy, D., Martens, P. C. H. & Yeates, D.A., 2010, ApJ, 720, L20.

Muñoz-Jaramillo, A., Nandy, D. & Martens, P. C. H. 2009, ApJ, 698, 461.

Muñoz-Jaramillo, A., Nandy, D. & Martens, P. C. H. 2011, Nature, 471, 80.

Schrijver, C. J., De Rosa, M. L. & Title, A. M., 2002, ApJ, 577, 1006.

Schrijver, C.J. & Liu, Y., 2008, SolP, 252, 19.

Švanda, M., Klvaňa, M., Sobotka, M. and Bumba, V. 2008, A&A, 477, 285.

Ulrich, R. K., 2010, ApJ, 725, 658.

Wang, Y. -M., Nash, A. G., Sheeley, N. R., Jr., 1989, Science, 245, 712.

Wang, Y. -M., Lean, J. L. & Sheeley, N. R., Jr., 2005, ApJ, 625, 522.

Wang, Y. -M., Robbrecht, E. & Sheeley, N. R., Jr., 2009, ApJ, 707, 1372.

Yeates, A. R., Nandy, D. & Mackay, D. H. 2008, ApJ, 673, 544